Chapter 3

The Relationship Between Arrhenius Pre-factors with Non-Covalent Binding
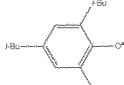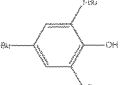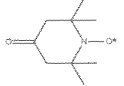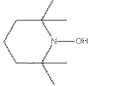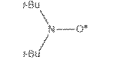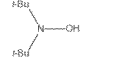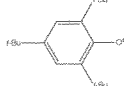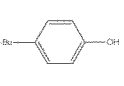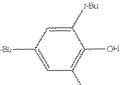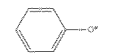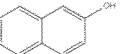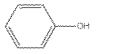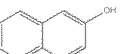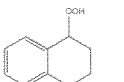
3.1 Introduction

DiLabio and Ingold[36] previously investigated the formal HAT reaction of the iminoxyl/oxime self-exchange reaction. In that paper, they compiled a table of parameters from the phenomenological Arrhenius equation for a series of interesting reactions, which appear here in Table 3.1.[40,127-133] These are thermoneutral hydrogen atom self-exchange reactions involving oxygen-centred radicals, and other nearly thermoneutral reactions involving the destruction and formation of oxygen-centred radicals, reactions 3.1 and 3.2, respectively:

$$\pi-RO^{\bullet} + ROH \longrightarrow ROH + \pi-RO^{\bullet} \qquad \Delta H = 0 \qquad (3.1)$$

$$\pi-R'O^{\bullet} + ROH \longrightarrow R'OH + \pi-RO^{\bullet} \qquad \Delta H \approx 0 \qquad (3.2)$$

Table 3.1: Table of results for (nearly) thermoneutral reactions studied. Units for ΔH, E_a, and calculated binding energy (BE) are kcal mol^{-1}, $\log A$ are log M^{-1}s^{-1}, and k are M^{-1}s^{-1}. References to the original literature are included with the Complex ID number. [†]Calculated binding energies involve structures which could not be fully optimized and contain one or more small imaginary frequencies. Adapted with permission from Reference 36. Copyright (2005) American Chemical Society.

ID	RO•/R′O•	ROH	ΔH	$\log A$	E_a	k	BE
1[40]			0.0	3.7	1.2	3.3×10^2	-10.8
2[127]			-2.0	3.8	3.8	10	-14.8
3[40†]			0.0	5.1	3.5	3.3×10^2	-10.1
4[128,129†]			4.2	5.5	4.8	93	-10.0
5[130]	t-BuOO•		-7.0	4.2	0.5	7×10^3	-6.5
6[40†]	Ph$_2$NO•	Ph$_2$NOH	0.0	>7	-	$>10^7$	-13.6
7[131]			-2.2	8.3	2.3	4×10^6	-8.6
8[132†]	t-BuOO•		0.3	7.2	5.2	3×10^3	-5.5
9[132†]	t-BuOO•		-1.9	6.4	2.6	3×10^4	-5.6
10[133†]	t-BuOO•		1.4	6.0	4.5	7×10^2	-8.0

Although it is well known that reactions of this nature involve remarkably low activation energies (E_a),[134–137] the Arrhenius pre-exponential factors (A), or as they shall be referred to herein, *A-factors*, as a well as rate

constants, span a wide range (summarized in Table 3.1): The measured A-factors range from $10^{3.5}$–$10^{8.3}$ $M^{-1}s^{-1}$ and the rate constants range from 10–10×10^7 $M^{-1}s^{-1}$. In the past, this range has been attributed to steric shielding around the oxygen atoms, resulting in a larger entropic barriers.[36] Importantly, it was noted that the degree of steric shielding on the oxygen atom appears to play an important role in the order of the A-factor; systems with greater bulk have lower A-factors, while non-shielded systems have larger A-factors.

Stereo-electronic effects are known to play an important role in HAT, and have been studied extensively.[38,138–144] Although the abstraction of a specific hydrogen atom may be more thermodynamically favourable than others on a given substrate, if it is not accessible due to steric constraints, abstraction will not occur at this site. Otherwise, additional steric bulk can lead to significant reductions in reactivity, through destabilization of the TS complex, or by forcing additional processes involving conformational changes in order to reach the appropriate TS structure. For example, in reactions of tertiary acetamides with $CumO^{\bullet}$,[144] where abstraction occurs mainly from C-H bonds α to the nitrogen atom, a two-fold decrease in the rate constant (normalized for the number of equivalent hydrogen atoms) is observed in going from N,N-dimethylacetamide to N,N-diisobutylacetamide ($k_H = 2.0 \times 10^5$ and 7.8×10^4 $M^{-1}s^{-1}$, respectively). The decrease in rate constant is attributed to the steric clash between the methyl groups of $CumO^{\bullet}$ and the isobutyl groups of N,N-diisobutylacetamide.

As all of the reactions in Table 3.1 are nearly thermoneutral, bond cleavage and formation will not play a significant role in determining the rate of

the effects of thermochemical effects on rates of reaction are expected to be minimal.

67

reaction. Therefore, the large degree of variance in their rate constants (k) is somewhat surprising. These reactions are closely related to the self-exchange reaction between phenol and phenoxyl,[23] in which a strong molecule-radical pre-reaction complex is formed, ca. 10 kcal mol^{-1} below the separated reactants. It is therefore expected that most, if not all, of the systems in Table 3.1 should exhibit a similar molecule-radical complex; granted, the strength of the interaction will vary because of steric repulsion. As such, it is plausible that the strength of this interaction may directly influence the rate of formal hydrogen atom transfer.

(BE in Table 3.1)

Currently, there has been no comprehensive investigation of the relationship between the pre-reaction complex and the kinetics of a reaction. On the basis of the reaction data in Table 3.1, we ask the question: *Do A-factors have a correlation with non-covalent binding energies of the pre-reaction complex?* This is a reasonable question as non-covalent binding and steric hinderance represent a loss of degrees of freedom and therefore entropy,[i] which ultimately determines the A-factor magnitude. If the answer to the question is yes, then non-covalent binding may be useful as a diagnostic for the "looseness" or "tightness" of a TS complex, in addition to providing an important link between theory and experiment.

3.2 Computational methods and details

Density-functional theory (DFT) calculations were carried out using the Gaussian-09 software package.[114] Care was taken to obtain minimum energy

---

[i] Recall from Equation 2.95 that the A-factor can be related to TST such that the primary variable is entropy ($\Delta^\ddagger S^0$).

structures through detailed conformational analysis. For this, the BLYP density-functional[100,145] was utilized, paired with the empirical D3 dispersion correction[107] with the recommended Becke-Johnson damping functions,[108] as well as our groups' own basis set incompletion potentials (BSIPs),[146] and minimal MINIs basis sets.[147] The use of minimal basis sets corrected for basis set incompleteness allows DFT-based methods (as opposed to semi-empirical or force-field based approaches) to be used efficiently in performing a large number of calculations. Minimum energy conformers of the monomers (substrates and radicals) were first obtained by manual manipulation of the necessary dihedral bond angles, followed by geometry optimization and vibrational analysis.

The lowest energy radicals and substrates were combined to generate the appropriate pre-reaction complexes. These pre-reaction complexes were subject to conformational analysis using the same BLYP-D3(BJ)-BSIP/MINIs method. Geometries were initially manipulated by hand. It became apparent that manual manipulation resulted in an unsatisfactory exploration of the conformational space. To solve this, all the necessary dihedral angles were scanned systematically using a combination of scripts.[148] All manipulated geometries were subject to optimization. For each complex, the top 5–10 complex geometries were subject to further optimization using a higher level of theory (BLYP-D3(BJ)-BSIP/pc-1) to obtain the final minimum energy pre-reaction complex structures. Due to the free rotation of groups such as *t*-butyl and methyl, some of the optimized pre-reaction complex structures contain small imaginary frequencies, and thus do not represent proper stationary states. Several measures were taken to resolve this, however,

no resolution was obtained in many cases. Regardless, the complexes adequately represent the pre-reaction complex and differences in "true" binding energies can likely be ignored.

To obtain accurate pre-reaction complex binding energies, the substrates and complexes were subject to single-point energy calculations using the LC-ωPBE long-range corrected density functional[149,150] with D3(BJ) dispersion corrections and pc-2 basis sets with truncated f-type functions (pc-2-spd).[151] This method was selected on the recommendation of work by Johnson et al.[151], which demonstrated the accuracy of this method for the calculation of NCIs. On the basis of the reported mean absolute error in Reference 151 for the S66 benchmark set of sixty-six different non-covalently interacting dimers,[152] the calculated binding energies reported herein from the LC-ωPBE-D3(BJ)/pc-2-spd level of theory carry an estimated 0.2 kcal mol^{-1} margin of error.

3.3 Results and discussion

The theoretically determined electronic binding energies calculated for the lowest energy pre-reaction complex of each system are listed in Table 3.1. The logarithm of A-factor against binding energy was plotted, as shown in Figure 3.1. The overall correlation is quite poor ($R^2 = 0.33$), however much of the data is grouped about a single, well correlated line ($R^2 = 0.95$). The intercept of the fitted line which corresponds to zero binding energy is 8.63, a value which is in line with what has been cited as the expected A-factor for HAT reactions, *viz.* $10^{8.5 \pm 0.5}$ M^{-1}s^{-1}.[153] These results suggest

that the observed correlation is genuine, that is, NCIs may have an impact on A-factors. I shall demonstrate that the data which do not correlate are reasonable outliers. In fact, using simple rationale I shall demonstrate that different regimes of steric bulk results in different mechanistic processes leading to the TS complex. As a result, deviations from the relationship between A-factor and binding energy are observed.
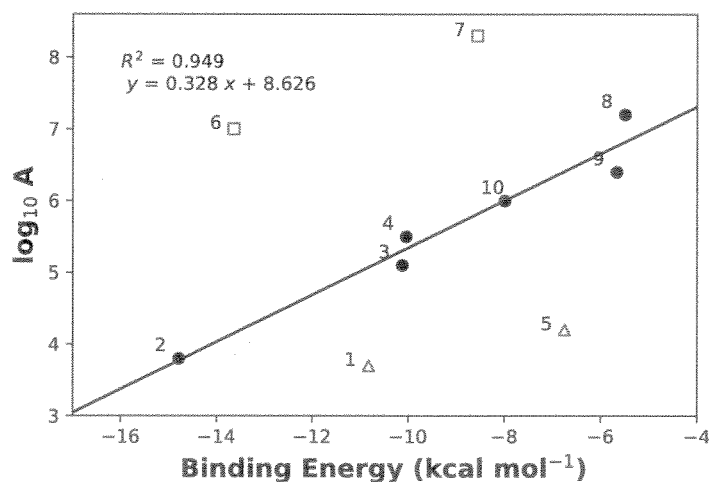

Figure 3.1: Plot of logarithm of A-factor against binding energy. Only the black points were included in the line fitting (slope = 0.328 kcal mol^{-1}, intercept = 8.626 kcal mol^{-1}, and R^2 = 0.949). Red points with open faced markers indicate outliers, *vide infra*. The inclusion of complexes 1, 5, and 7 result in an R^2=0.334. Complex 6 is always omitted from line fitting as the experimental A-factor is approximate.

In order to illustrate this, consider the fundamental properties of the HAT reactions involved herein. There are two important concerted reaction mechanisms that are possible, namely direct HAT or PCET. Recall that in 1, the notion was introduced that the rate constant (and thus A-factor) for

formal HAT (k_{HAT}) can be described as a combination of the rate constants direct HAT (k_{direct}) and PCET (k_{PCET}) mechanisms, i.e.:

$$k_{HAT} = k_{direct} + k_{PCET} \tag{3.3}$$

Although the distinction between these two mechanisms is somewhat poorly described, this concept can be used to described the deviations from the expected trendline herein.

Specifically, we must consider the geometric constraints in which these reaction mechanisms occur. For direct HAT to occur, the SOMO of the radical must overlap with the O-H σ^* anti-bonding orbital. This may require the rotation of the hydrogen atom donating hydroxyl group out of the plane. The rotation of a phenolic hydroxyl group has an energy barrier that follows a $\cos^2 \theta$ relationship,[154] and can be as high as 3.1 kcal mol^{-1} on the basis of the rotational barrier in phenol.[155] For a PCET mechanism to occur, there are two possible geometries: Either the SOMO of the radical overlaps can overlap with the corresponding oxygen (LP) p-orbital, as seen in the work of Mayer et al.[23]. Note that in this case direct HAT cannot occur due to geometric constraints, and thus $k_{direct} = 0$ and $k_{HAT} = k_{PCET}$.

Alternatively, a LP-π, LP-LP, or π-π bonding overlap between the radical and substrate can occur, as seen in the work of DiLabio and Ingold[36], and DiLabio and Johnson[26]. Furthermore, I shall suggest that although PCET can occur due to different types of orbital interactions, the net contribution to k_{HAT} from PCET is likely not equivalent in all cases. It is reasonable to state that π-electrons are more easily delocalized than LP-electrons.

72

Therefore, the strength of π-π bonding interactions can be described as the strongest, while LP-π interactions are weaker and LP-LP interactions are weakest. This suggests that the contributions of k_{PCET} are greatest in the case of π-π bonding interactions, less for LP-π interactions, and least for LP-LP interactions. Herein, I maintain a focus on pre-reaction complexes, the geometries of which allow the estimation of the TS complex structures. By applying these basic principles, it is possible to rationalize deviations from the trend observed in Figure 3.1.
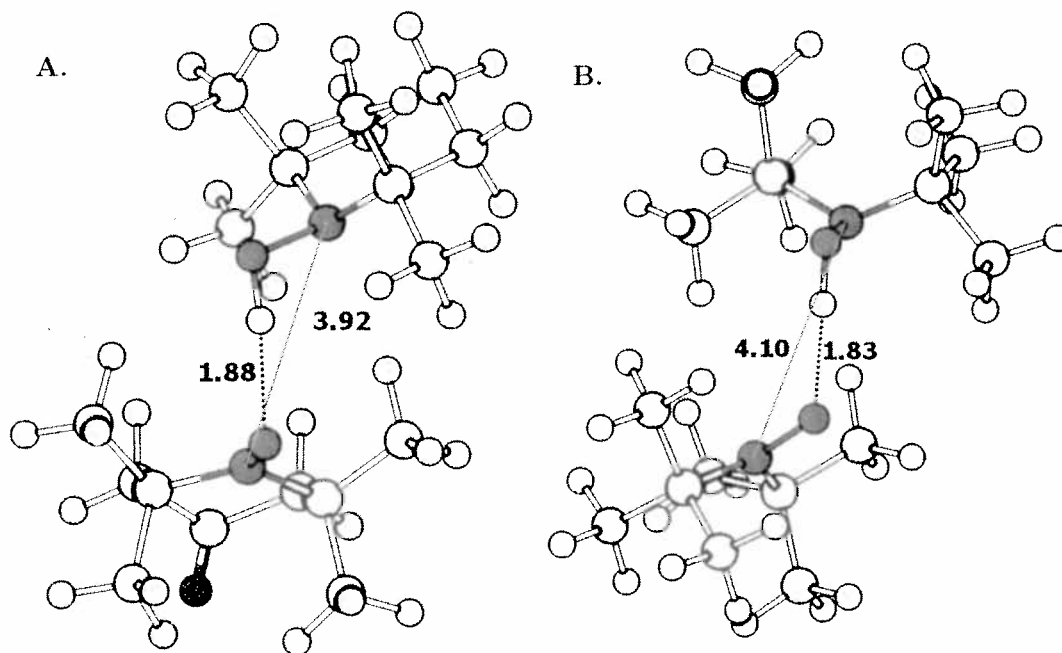
A.

B.

3.92

1.88

4.10 1.83

Figure 3.2: Three-dimensional structures of **A** complex 2 (TEMPO-H and 4-oxo-TEMPO) and **B** complex 3 (di-*t*-butyl-hydroxylamine and di-*t*-butyl-nitroxyl). Hydrogen bond distances are shown in units of Å. The elements are coloured as white for carbon, light blue for hydrogen, red for oxygen, and blue for nitrogen.

I shall begin by examining the points which fall on the expected line, complexes 2–4 and 8–10. The examination of all these pre-reaction complexes reveals that an additional rearrangement that has a moderate energetic barrier is required in order for ~~formal HAT reactions~~ *the hydrogen transfer* to proceed. Complexes 2 and 3 are shown in Figure 3.2, and are very similar in structure. Both are hydroxylamine-nitroxyl couples with similar degrees of steric bulk adjacent to the reacting centres. The *t*-butyl groups of 3, and the methyl groups of 2 prevent the alignment of the NO-H-ON frameworks for PCET. Thus, while the TS structure may have some degree of LP-LP bonding interaction, the overall mechanism is dominated by direct HAT.

can you report the dihedrals?

Which are ideal for PCET is

In the most stable stacked conformation, complex 4, as seen in Figure 3.3, steric clash of the para-position *t*-butyl groups obstructs π-π overlap between the aromatic rings. It is likely that this steric clash does not allow any significant orbital interaction, ~~thus this~~ *suggesting that the* reaction is dominated by direct HAT. In order to react via direct HAT, the hydroxyl group must rotate further out of the aromatic plane, or the bulky para-position *t*-butyl groups must come into close proximity. Alternatively, an open conformation for complex 4 is possible, which lies ca. 2 kcal mol^{-1} higher in energy than the stacked complex, a result which is also consistent with the observed trend-line. From the open conformation, PCET is still not possible due to the steric bulk of the ortho-position *t*-butyl groups of the radical, thus this reaction likely also proceeds through a direct HAT mechanism.

Complexes 8 and 9 are similar systems, in which t-BuOO$^\bullet$ reacts with unhindered phenolic substrates. As seen by the structures in Figure 3.4, the bound complexes are somewhat dissimilar. The hydroxyl group of com-

Figure 3.3: Three-dimensional structure of pre-reaction complex 4 between 2,4,6-tri-*t*-butylphenol and 4-*t*-butylphenoxyl. **A** demonstrates the hydrogen bond distances in units of Å, and the out-of-plane rotation by 35.2° of the phenolic hydroxyl group. **B** demonstrates the steric clash (highlighted by red box) between the para-position *t*-butyl groups. The elements are coloured as white for carbon, light blue for hydrogen, and red for oxygen.

plex 8 is rotated out of the plane 24°, while in complex 9 the hydroxyl group lies entirely in the plane. It is likely that the larger aromatic system of 2-naphthol results in a larger OH rotational barrier, and thus the most favourable conformation is entirely in the plane. In complex 9, there is also a weak hydrogen bond between the C-H bond in the ortho-position and the non-radical O-centre of $t-$BuOO$^\bullet$, contributing further to the stabilization of the planar conformation. Complex 8 was previously studied by DiLabio and Johnson[26], where it was demonstrated that a partial bonding *in the TS* interaction exists between the peroxyl LP and phenolic π-system. However, this interaction is likely weak thus contributes weakly to the overall rate constant. That is, k_{HAT} is dominated by k_{direct}. Also, although the pre-reaction complexes are somewhat dissimilar, the conformational changes necessary to reach the TS complex, similar to that reported in reference 26, are likely not dramatically different in terms of energetic barriers. Any small differences result in noise in the observed trend.

Complex 10, shown in Figure 3.5 is unique in that it is the only reaction between a peroxide and a peroxyl radical. Therefore, this system represents the best case scenario for LP-LP overalap to occur. The self-exchange reaction between HOO$^\bullet$ and HOOH can be considered the simplest reference for the reaction of α-tetralin peroxide with t-butylperoxyl. To the best of my knowledge, the mechanism of the hydroperoxyl-hydrogen peroxide couple has not been characterized as either PCET or direct HAT previously in the literature, although the TS structure has been previously reported.[156] Using this structure, calculations reveal a LP-LP interaction leading to partial bonding in the TS, i.e. a PCET mechanism. (See Appendix A, Figure A.1).
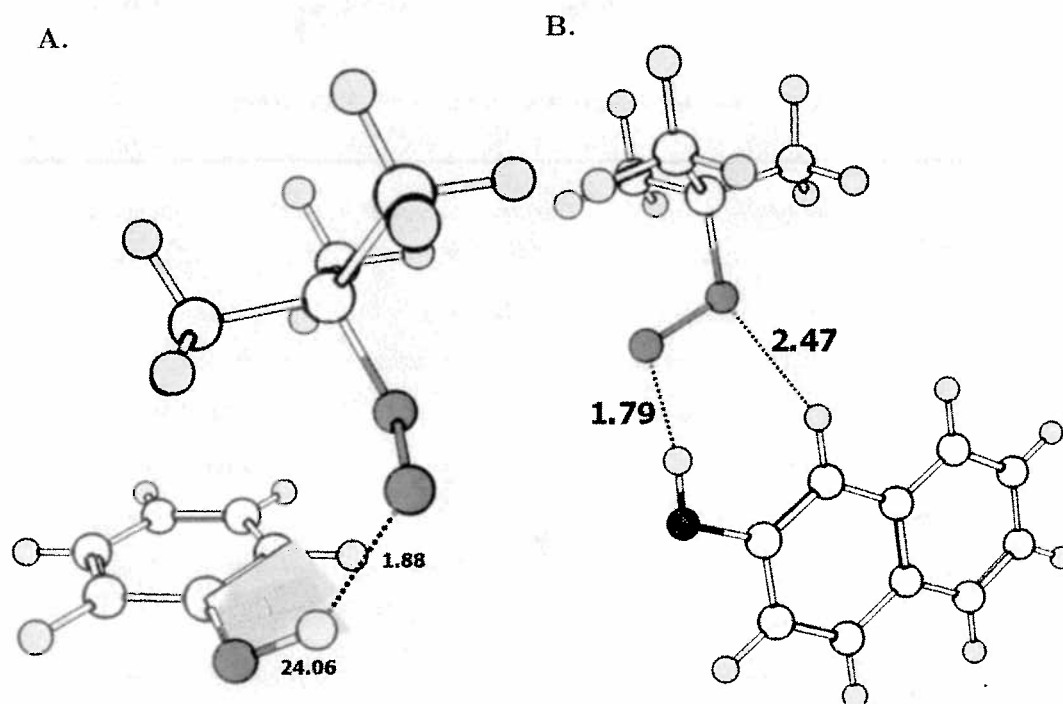
76

Figure 3.4: Three-dimensional structures of pre-reaction **A** complex 8 (*t*-butylperoxyl and phenol) and **B** complex 9 (*t*-butylperoxyl and 2-naphthol). Hydrogen bond distances are shown in units of Å. Complex 8 has an out of plane rotation of the phenolic hydroxyl group of 24.1°. The elements are coloured as white for carbon, light blue for hydrogen, and red for oxygen.

The hydroperoxyl-hydrogen peroxide couple contains a H−O−O−H dihedral angle of 90°, so that the two non-reacting hydrogen atoms oriented 180° away from one another. Orienting substituents directly away from one another is likely the most stable TS structure for all peroxyl-peroxide formal HAT reactions.

Complex 10 is unlikely to orient t-butylperoxyl and α-tetralin peroxide exactly 180° away from one another due to steric clash. Nonetheless, there may still be some LP-LP overlap contributing to a weak k_{PCET} contribution to k_{HAT}. On the basis of the line fit in Figure 3.1, and given that the other point are dominated by k_{direct}, the same is likely true in the case of complex 10. This means that either the TS structure does not allow for sufficient LP-LP overlap for k_{PCET} to dominate, or LP-LP overlap does not allow for a strong PCET contribution to k_{HAT}. This will require additional investigation.

Once again, complexes 2–4 and 8–10 follow the observed trend. In all cases, these complexes may have some PCET contribution to k_{HAT} through either LP-π or LP-LP orbital overlap. Interpretation of Figure 3.1 in this manner allows for two possible explanations. The simpler is that all these complexes proceed through a mechanism in which $k_{HAT} \approx k_{direct}$ ($k_{PCET} \ll k_{direct}$). In this case, the A-factor is a direct reflection of k_{HAT} and this the pre-reaction complex binding energy correlates well with the A-factor.

Alternatively, there may be increasing contributions of PCET leading to an increase in the A-factor. This effect can be rationalized on the basis of a stronger interaction in the case of LP-π overlap, as compared to LP-LP overlap. Within this framework, complexes 2, 3, and 4 may have little or no
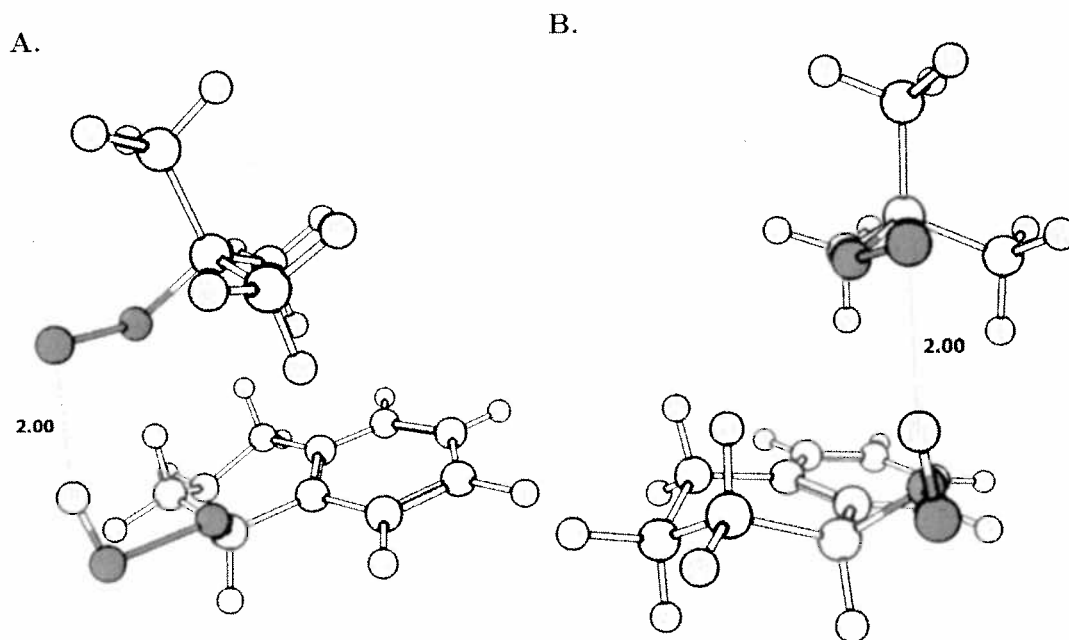
Figure 3.5: Three-dimensional structure of pre-reaction complex 10 between *t*-butylperoxyl and α-tetralin peroxide. **A** demonstrates the hydrogen bond distances in units of Å. **B** demonstrates the likely steric clash preventing strong LP-LP overlap. The elements are coloured as white for carbon, light blue for hydrogen, and red for oxygen.

overlap due to steric clashing, ~~which~~ complex 8 and 9 have a higher A-factor
and es
than complex 10 due to LP-π vs. LP-LP overlap. Further work is necessary
to ~~disseminate~~ this effect.
discern

Consider next the points which sit above the trendline, complexes 6
and 7, shown in Figure 3.6 and Figure 3.7. The A-factor for complex 6 is
approximate and thus does not get factored into the line fitting. In both
cases, the non-covalently bound complexes are in a slipped-parallel π-stacked
conformation, allowing for π-π orbital overlap. Complex 7 in particular is
very similar to the phenol-phenoxyl couple, except with 2-naphthol instead
of phenol. Therefore, it is possible to infer that both of these reactions take
place through mechanism in which k_{PCET} is dominant. The key difference
from the points which fall on the trendline is that $k_{HAT} \approx k_{PCET}$.

Lastly, consider the points which fall below the trendline, complexes 1
and 5. In both cases, a high degree of steric repulsion likely does not allow
for a PCET mechanism through orbital overlap. It is important in to study
the "encounter complex" which represents the first pre-reaction complex, i.e.
prior to any reorganization, as this will be that which is affect the A-factor
with regards to simple collision theory. Complex 1 is the self-exchange reac-
tion between the very bulky 2,4,6-tri-*t*-butylphenol/2,4,6-tri-*t*-butylphenoxyl
couple, as seen in Figure 3.8 A. As a result of steric shielding around the
reaction centres, the encounter pre-reaction complex is stacked to maximize
dispersion interactions, but does not have a hydrogen bond. Therefore, ~~these~~
must be a higher-energy hydrogen-bonded pre-reaction couple that leads to
the direct HAT mechanism. Note however, that there is a barrier to rotation
of the hydroxyl group to 90° out of the plane for direct HAT to occur.

the T-stacked
1PRC is
very close to
the presumptive
π-stack TS.

an addition
rearrangement
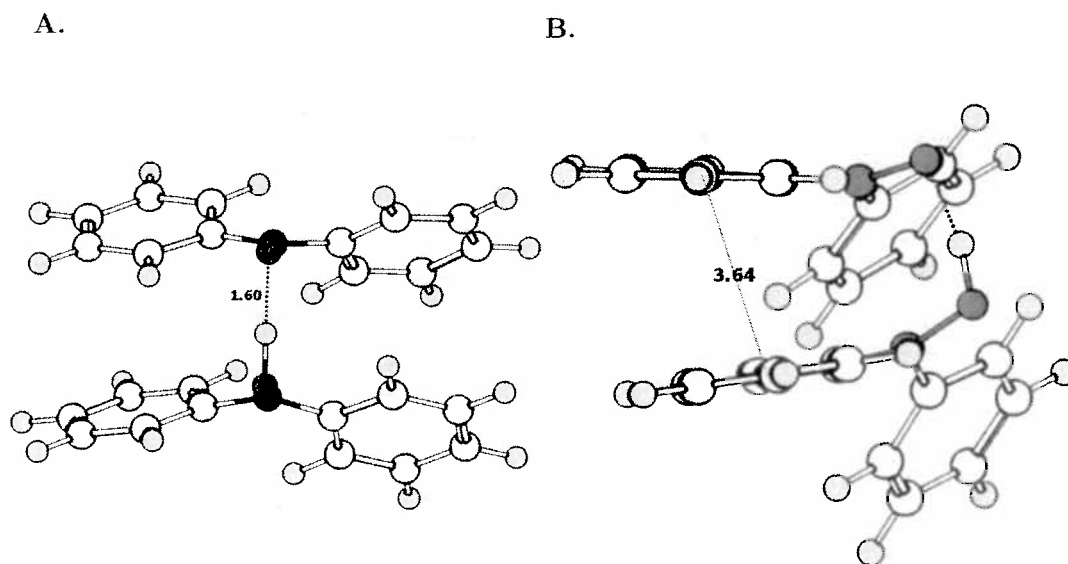*is required*
in order to get
to the TS

Figure 3.6: Three-dimensional structures of pre-reaction complex 6 between N, N-diphenylhydroxylamine and N, N-diphenylnitroxyl. **A** demonstrates the hydrogen bonding interaction while **B** demonstrates the π-π interaction. Distances in unit of Å and angles are shown in degrees. The elements are coloured as white for carbon, light blue for hydrogen, blue for nitrogen, and red for oxygen.
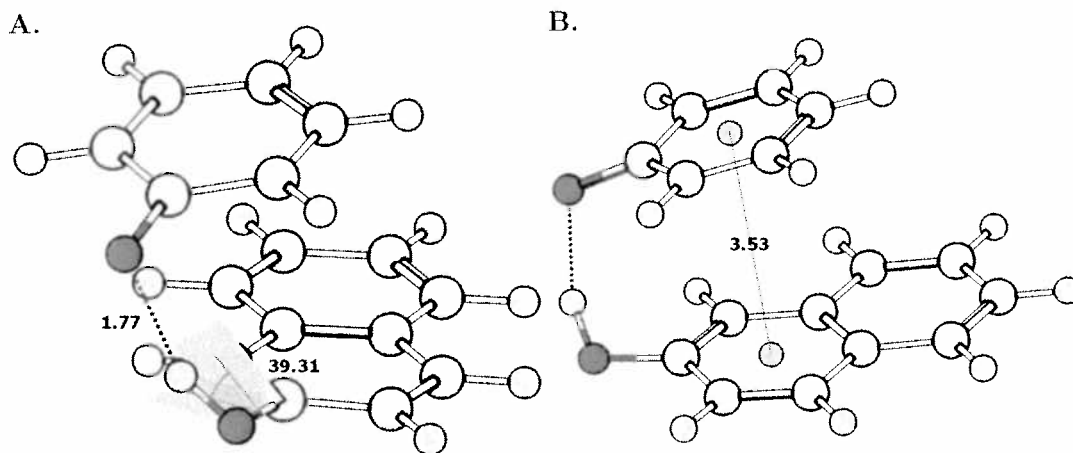
Figure 3.7: Three-dimensional structures of pre-reaction complex 7 between 2-naphthol and phenoxyl. **A** demonstrates the hydrogen bonding interaction while **B** demonstrates the π-π interaction. Distances in unit of Å and angles are shown in degrees. The elements are coloured as white for carbon, light blue for hydrogen, and red for oxygen.

Complex 5 is the 2,4,6-tri-t-butylphenol/t-butylperoxyl reaction couple. The encounter pre-reaction complex also does not contain a hydrogen bond. As with complex 1, an encounter pre-reaction complex without a hydrogen bond must form first. However, in complex 5 there is less steric clashing. As a result the formation of a hydrogen bond is favourable and the "true" pre-reaction complex is about 0.7 kcal mol^{-1} more stable than the encounter complex. In contrast, for complex 1 the true pre-reaction complex is about 0.6 kcal mol^{-1} less stable than the encounter complex. Note also that there is a barrier to rotation[ii] of the hydroxyl group that can be estimated as about 4.1 kcal mol^{-1}. This is illustrated schematically in Figure 3.9.

[ii]Calculated as the difference in energy between the in-plane and out-of-plane structures of 2,4,6-tri-t-butylphenol at the LC-ωPBE-D3/6-311+G(2d,2p) level of theory.
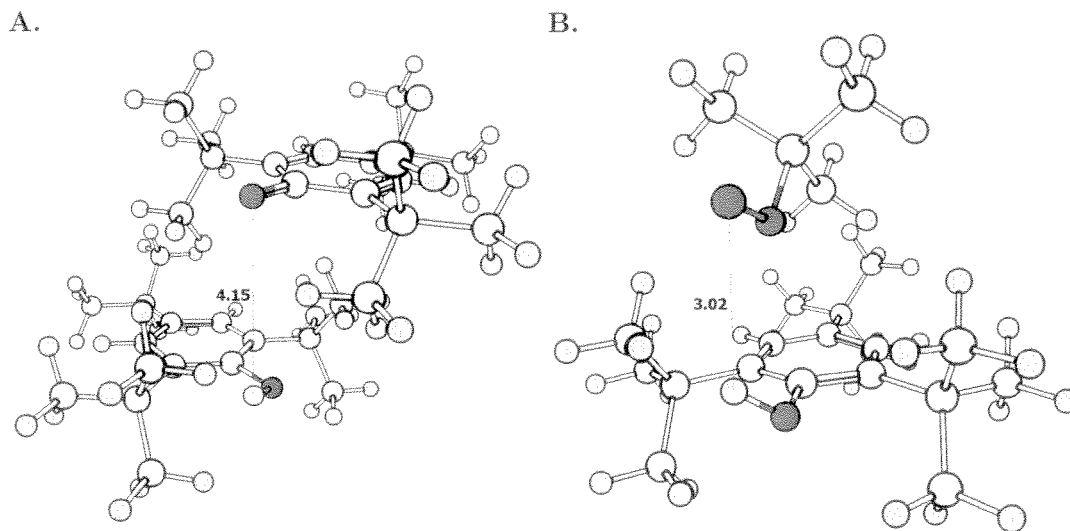
A.
B.

Figure 3.8: Three-dimensional structures of pre-reaction **A** complex 1 (2,4,6-tri-*t*-butylphenoxl and 2,4,6-tri-*t*-butylphenoxyl) and **B** complex 5 (2,4,6-tri-*t*-butylphenol and *t*-butylperoxyl). Distances in unit of Å and angles are shown in degrees. The elements are coloured as white for carbon, light blue for hydrogen, and red for oxygen.
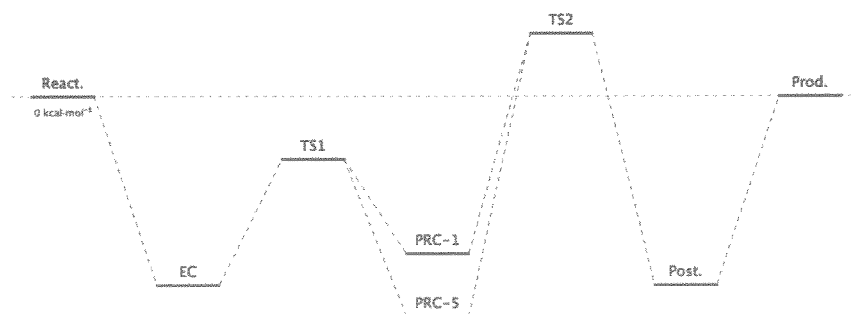

Figure 3.9: Reaction coordinate illustrating proposed mechanism for HAT in complexes 1 and 5. React. = reactants, EC = encounter complex, PRC-1/5. = true pre-reaction complex 1/5, TS = transition state, Post. = post-reaction complex, Prod. = products.

TS1 indicates the TS associated with out-of-plane rotation of the OH group. TS2 represents the (presumptive) TS associated with HAT.

For both complex 1 and 5, steric clashing prevents significant π-π overlap or LP-π overlap. Therefore, the reactions likely proceed through a direct HAT dominated mechanism ($k_{HAT} \approx k_{direct}$). One might then expect these data to fall on the trendline, however the formation of an encounter complex which does not lead directly to HAT results in a different overall process from the other complexes. As a result of the necessary initial process complex 1 and 5 have lower A-factors as less collisions are likely to lead to successful formal HAT.

3.4 Summary

In this investigation, a series of thermoneutral or nearly thermoneutral HAT reactions were considered. I have plotted the theoretically determined electronic binding energies against the logarithm of experimentally determined A-factors. These results demonstrate that the A-factors for (nearly) thermoneutral HAT reactions correlate to some extent with the pre-reaction complex binding energies, given that the reactions proceed through similar mechanisms and energetically similar pathways. The results herein can be sorted into three bins by considering the contributions of k_{direct} and k_{PCET} to the overall transformation, k_{HAT}:

1. Complexes which have weak k_{PCET} contributions due to either LP-LP or LP-π orbital overlap, and are therefore dominated by k_{direct}. This is the case for the data which fall on the trendline.

2. Complexes in which k_{PCET} is the dominant contribution to k_{HAT}, as

is the case for complexes 6 and 7.

3. Complexes in which the encounter complex does not lead directly the the HAT TS complex, as was the case for complexes 1 and 5.

These results indicate that different regimes of electronic and steric interactions lead to different chemical processes in seemingly similar reactions. As a results, non-covalent binding can be used as a metric for kinetics parameters, however, it cannot describe in full the entropic factors which contribute to the A-factor. One must first consider the mechanistic details in which formal HAT occurs.

Additional work is necessary to extend these results. In particular, the main question which remains is whether π-π PCET is "better" than other forms of orbital overlap. To answer this a larger sample of data points, and a diagnostic for PCET must be used. Regardless, the results herein represent a novel attempt to link theory and experiment. Given that obtaining the full PES for large molecules is currently computationally impractical, these results serve as a seed for developing a fundamental understanding of complex formal HAT reactions.

Chapter 3

- remains somewhat difficult to understand, in particular because the ideas around A-factor & rate constant are being convoluted.

One way to address this is to first discuss the nature of the reactions via HAT or PCET[*], then to talk about the role played by the pre-reaction complex (PRC) or the association complex. After this, the description of the three types of PRCs is straight forward.

- I would avoid making presumptive statements around the strengths of interactions (eg. bottom of pg 72, top of 73). In addition, it is unclear what these interactions refer to (ie. TS or PRC). In the PRC, these $\pi-\pi$, $LP-\pi$, etc. are weakly attractive, dispersive forces. In the TSs, they allow for bonding, & therefore the formation of a channel for e^- transfer.

[*] Note that it is unclear from recent literature (eg. Hammes-Schiffer) that PCET means the same to us as it to them. However, if we

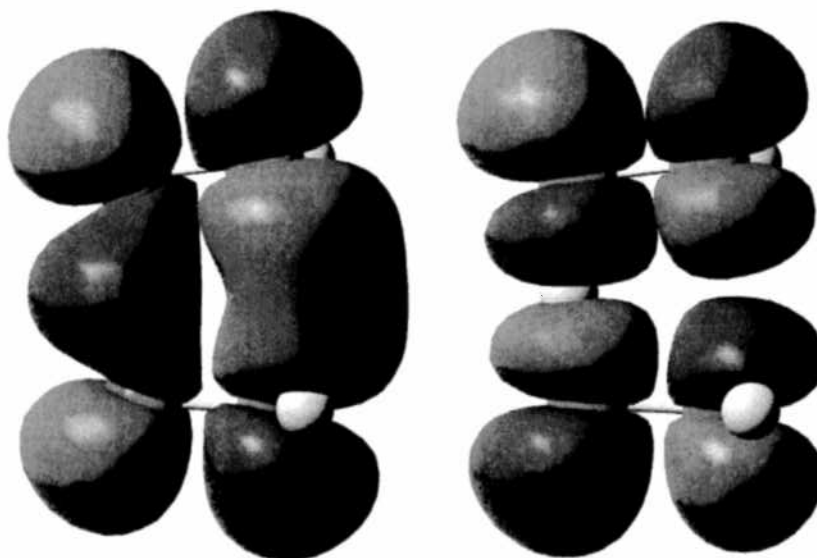# Appendix A

Chapter 3 Additional Data

Figure A.1: Molecular orbitals of hydrogen peroxide-peroxyl self-exchange reaction TS complex, demonstrating a PCET mechanism. Left is the HOMO-1 and right is the SOMO. Together they demonstrate a lone pair-lone pair net half bonding interactions, consistent with PCET. MOs are shown with an isovalue of $0.02\ e^-/\text{Å}$.